

Mass transfer characteristics from a rotating cylinder

Ma H.T.*, Zhang Y.F., and Deng N.

*Author for correspondence

Department of Building Services Engineering,
School of Environmental Science and Technology,

Tianjin University,

Tianjin 300072, China(RC)

E-mail address: mht116@tju.edu.cn

ABSTRACT

Mass transfer characteristics from a large diameter horizontal rotating cylinder are investigated experimentally. The local mass transfer coefficient h_φ and the average mass transfer coefficient h are measured by using a specialized minitype dry and wet bulb thermocouple and a calorimeter. On the base of experimental data, some equations correlating the average Sherwood number (Sh) and the critical Reynolds number ($Re_{r,cri}$) with parameters of Re_r , Gr , and Sc have been obtained. The results are: $Sh = 0.32[(8.5 Re_r^2 + Gr) \cdot Sc]^{1/3}$ and $Re_{r,cri} = 0.44(Gr \cdot Sc)^{1/2}$, respectively.

INTRODUCTION

Rotating cylinders are used in most cases when high transport coefficient is required. There are numerous examples of industrial applications where rotation plays important roles in mass and heat transfer as convective media, such as drying of textiles, film materials and paper, corrosion of electrode, electrochemical deposition, and so on. Labraga and Berkah [1] investigate the local mass transfer from a rotating cylinder with and without crossflow by using the electrochemical technique, the results shows that the upstream moving surface of the rotating cylinder contribute the most to the mass transfer enhancement, and the heat transfer process can be predicted accurately by heat and momentum transfer analogy for a rotating cylinder in a quiescent fluid. The study on the characteristics of heat transfer from a rotating cylinder by X. M. Zhang et al[2] indicates that as long as the rotational speed is below the critical ones, the heat transfer is independent of the rotation speed. There exist

several experimental investigations for the characteristics of the electrode corrosion and electrochemical deposition of cupric ions from either vertical or horizontal cylinders[3-5]. A study of transport mechanisms of turbulent flow and scalar transport in the straight pipe and rotating cylinder has been made numerically and experimentally[7]. Fouad A.Youssef[8] studies the problem of heat transfer from an impulsively started translating and expanding circular cylinder analytically using the method of matched inner-out expansion to the third order. F. Gori and L.Bossi[9] study the optimal slot height in the jet cooling of a circular cylinder. The experimental results are presented of heat transfer cooling of electrically heated circular cylinder, the average and local Nusselt numbers are presented versus the Reynolds number, the distance of the cylinder from the slot exit and the angle from the impinging point. However, the study of convective mass transfer from the porous medium wall of a large diameter horizontal cylinder has not been reported up to now. Therefore, the main purpose of the present experiment is to provide detailed experimental data to illustrate the characters of mass, by which the mass transfer relationships of average Sherwood number Sh and critical Reynolds number $Re_{r,cri}$ can be better understood. These equations are supposed to be supportive and helpful for the further research and engineering design in this field. It also provides a good method of enhancing the heat and mass transfer coefficient and improving the technology for a rotating cylinder.

NOMENCLATURE

Re_r , [-] rotational Reynolds number, $n\pi d^2 / 60\nu$

Sh	[-]	average Sherwood number, hd/D
Sh_ϕ	[-]	local Sherwood number
h	[m/s]	average convective mass transfer coefficient
h_ϕ	[m/s]	local mass transfer coefficient
Sc	[-]	Schmidt number
Gr	[-]	Grashoff number
Ra	[-]	Rayleigh number, $Gr \cdot Sc$
$Re_{r,cri}$	[-]	critical rotational Reynolds number
D	[m ² /s]	mass diffusion coefficient vapor in air
d	[m]	diameter of the porous medium cylinder
r_0	[m]	radius of the porous medium cylinder
r	[m]	the distance between the measuring point and the cylinder axes
y	[m]	the distance between the measuring point and the front of the porous medium cylinder
n	[rpm]	rotational speed of the cylinder
m	[kg/m ² s]	mass flux
t	[°C]	dry bulb temperature
t_s	[°C]	wet bulb temperature

Greek symbols

ϕ	[-]	relative humidity
ρ	[kg/m ³]	density of vapor
ν	[m ² /s]	kinematic viscosity
λ	[W/m.°C]	thermal conductivity
ρ^+	[-]	dimensionless density, $(\rho - \rho_f)/(\rho_w - \rho_f)$
y^+	[-]	dimensionless distance, y/r_0
θ	[-]	dimensionless temperature, $(t - t_f)/(t_w - t_f)$

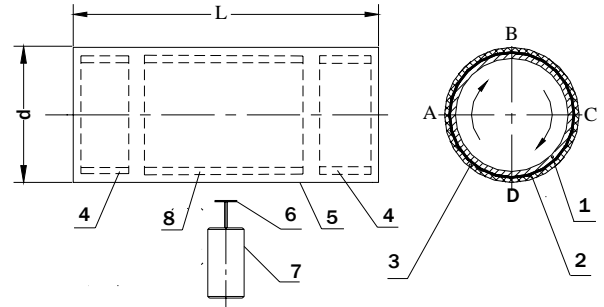
Subscripts

cri	critical state; sv saturation state
f	surrounding conditions
w	cylinder wall conditions
ϕ	circle angle

EXPERIMENTAL DETAILS

Fig.1 is the experiment configuration, the diameter of the cylinder is 315mm, and the length of the cylinder is 800mm.

In order to measure the average convective mass transfer coefficient h and the average Sherwood



1-the wall of cylinder; 2-silicon rubber sheet; 3-absorbent cotton fabric; 4-assistant heater; 5-rotating cylinder; 6-detector probe; 7-contral motor; 8-main heater
Fig.1 Schematic of the experimental facility

number Sh , the method of calorimeter made from silicon rubber sheet is applied to measure the vaporizing heat flux. First, the silicon rubber sheet (1mm thick) is pasted onto the cylinder surface, then the absorbent cotton fabric is enlaced outside the silicon rubber sheet, so that the outside diameter of the cylinder increases to 320mm. Five thermocouples with diameter of 0.1mm are embedded into the metal wall (0.1mm under the surface). Three are located at the middle sect of the cylinder and two are adjacent to the both ends. Consequently, the temperature distribution of the cylinder wall can be measured momentarily, and the measured temperature measure can be taken as the inside temperature of the silicon rubber sheet. Four more thermocouples with diameter of 0.08 are installed: two in the clearance between the silicon rubber sheet and the absorbent cotton fabric, and two inside the absorbent cotton fabric. All are aligned on the same radial line. Therefore, the temperature difference between the inside and the outside of the silicon rubber sheet, as well as the temperature in the absorbent cotton fabric can be measured and calculated. The data acquisition system includes a mercury slipringless transmitter that performs the coupling of electrical signals from the rotating parts to non-rotating surroundings. The voltage output from the thermocouples was at first amplified was then digitized and sampled by a Personal Computer. In a constant mass transfer state, the heat flux through the absorbent cotton fabric can be calculated based on the temperature difference of the silicon rubber sheet. The thermal conductivity of the silicon rubber plate λ is given as follows:

$$\lambda = 0.2473 - 3.2794 \times 10^{-4} t \text{ W/m.}^\circ\text{C} \quad (1)$$

Equation (1) shows that the thermal conductivity of the silicon rubber sheet λ varies slightly with

the temperature. The mass flux m can be calculated from the vaporizing heat flux q , which can be obtained from the conductive heat flux q_λ after deducting the radiant heat q_r and convective heat q_c . The average convective mass transfer coefficient h can be derived as follows:

$$h = m / \Delta\rho = m / (\rho_w - \rho_f) \quad (2)$$

where m is the mass flux of water through the porous medium, and $\Delta\rho$ is the difference between the density of vapor at the cylinder wall and the density of vapor in the surrounding, that is $\Delta\rho = \rho_w - \rho_f$.

The average Sherwood number Sh is derived from the equation as below:

$$Sh = hd / D \quad (3)$$

where D is the diffusion coefficient vapor in air, and d is the diameter of porous medium cylinder.

In the present experiment, the amount of the radiant heat q_r and convective heat q_c accounts for approximately 20% of the conductive heat flux q_λ . Therefore, how to measure the temperature difference of the silicon rubber sheet is important to h and Sh .

Fig.2 shows the disposal of the thermocouples in different parts of the cylinder wall, the thickness of cylinder metal wall is 5mm, the silicon rubber sheet is 1mm thick, and the absorbent cotton fabric is 1.5mm thick. There are five thermocouples that are embedded 1mm deep inside the cylinder metal wall, two are impacted outside the silicon rubber sheet by the pledget. The temperature differences of the three

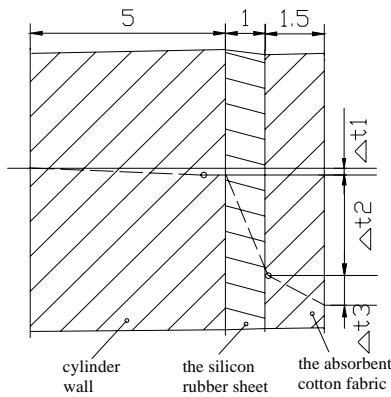


Fig.2 The schematic of temperature differences of the different layers from the cylinder wall

layers are represented as Δt_1 , Δt_2 , and Δt_3 respectively. Since the thermal conductivity λ of the silicon rubber sheet is much smaller than the ones of the metal cylinder and the pledget, Δt_2 is expected to be much larger than Δt_1 and Δt_3 , the temperature distributions of Δt_1 , Δt_2 and Δt_3 are shown in Fig.2.

For example, when the conductive heat flux $q_\lambda = 2475W/m^2 \cdot h$, $\Delta t_2 = 10.4^\circ C$, $\Delta t_3 = 1.5^\circ C$, and $\Delta t_1 = 0.28^\circ C$ respectively. In the condition of this experiment, the measurement error of Δt_2 is approximately +3%.

In order to obtain the dry and wet bulb temperatures in boundary layer, a special fine thermocouple measurement instrument is designed and used in the experiments. The configuration is shown in Fig.3.

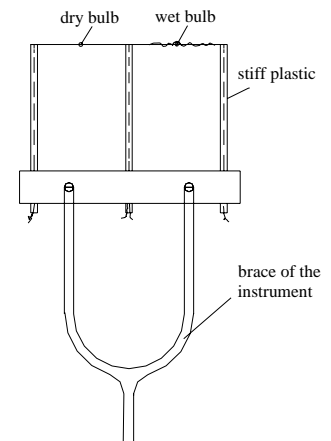


Fig.3 Schematic of the minitype dry and wet bulb thermocouples

The diameters of the dry and wet bulb thermocouples are all 0.05mm, they both are 20mm long, and are placed in a horizontal and parallel manner. The distance between the thermocouple and the front of the cylinder wall is controlled by a microcomputer. In order to eliminate the disturbance of the wet bulb to the boundary layer, the bulb's volume has been made as small as possible. Only several threads of cotton are wrapped around the thermocouple so that a thin moisture film is maintained on the web bulb, the outside diameter ranges from 0.2 to 0.3mm. The experimental data has been rectified against the affect of radiation.

The rotational speed of the cylinder n is counted by a photoelectric counter, in the meantime, the measured data is collected and printed, its

absolute error is $\pm 1/10$ revolution per minute.

By using the special detector, the local convective mass transfer coefficient h_ϕ and local Sherwood number Sh_ϕ can be calculated from the measured dry and wet bulb temperatures. According to the experimental data, the effect of the rotation on the mass transfer at different circle angle (ϕ) can be determined. In the mean time, the characteristics of the h and Sh varying with rotational Reynolds number Re_r are also investigated by means of the method of calorimeter made from silicon rubber sheet for different mass flux m . The convective mass transfer equations relating the average Sherwood number Sh with the Reynolds number Re_r , *Grashof* number Gr , and *Schmidt* number Sc are derived from the experimental data. The discriminant of critical rotational Reynolds number $Re_{r,cri}$ is also obtained.

Prior to the experiment, the absorbent cotton fabric is soaked with hydronium water. At a constant rotate, the cylinder wall temperature arises during the first period, then it changes slightly, when the mass transfer gets into a constant state (about an hour), the experimental data are collected (usually every several minutes). The temperature difference during the constant mass transfer period is only $1.25^\circ C$, which is accurate enough to the measurement. During the constant drying rate period, the temperatures at different parts (see Fig.2.) are independent on the original moisture content in the porous medium. The measuring process is implemented at a constant wall temperature and with a constant vapor creation. In this present experiment, the temperature of the porous medium cylinder wall varies from $30-70^\circ C$, the rotational Reynolds number Re_r from $2 \times 10^3 - 6 \times 10^4$, the *Grashof* number Gr from $5.3 \times 10^8 - 1.5 \times 10^9$, and the boundary layer is in a turbulent state.

Based on the measured dry and wet temperatures, the relative humidity can be calculated from the equation (4) as below[10]:

$$\phi = \frac{A_s - 1.005(t - t_s)}{A - [A - A_s + 1.005(t - t_s)]P_{sv}(t)/P_a} \quad (4)$$

where

$$A = \frac{P_{sv}(t)}{P_a - P_{sv}(t)} (1556 + 1.156t - 2.604t_s)$$

$$A_s = \frac{P_{sv}(t_s)}{P_a - P_{sv}(t_s)} (1556 - 1.448t_s)$$

$$p_{sv}(t) = p_{cv} \exp\left\{7.21275 + 3.981\left(0.745 - \frac{t + 273.15}{647.3}\right)^2 + 1.05\left(\frac{t + 273.15}{647.3}\right)^3 \cdot \left(1 - \frac{647.3}{t + 273.15}\right)\right\}$$

The equation leads to the expression relating the density of vapor ρ to the density of saturation vapor ρ_{sv} of:

$$\rho = \phi \rho_{sv} \quad (5)$$

where t and t_s are the dry and wet temperatures in the boundary layer; P_{cri} and P_{sv} are the critical and saturation pressure of vapor; P_a is the ambient pressure; ρ is the vapor density at the temperature t in the boundary layer, ρ_{sv} is the saturation vapor density at the temperature t in the boundary layer.

The local convective mass transfer coefficient h_ϕ and local Sherwood number Sh_ϕ can be derived from the *Navier - Stokes* equations:

$$h_\phi = \frac{D}{\Delta\rho} \left(\frac{\partial\rho}{\partial R}\right)_{r=r_0,\phi} \quad (6)$$

$$Sh_\phi = \frac{h_\phi d}{D} = \frac{d}{\Delta\rho} \left(\frac{\partial\rho}{\partial r}\right)_{r=r_0,\phi} = 2 \left(\frac{\partial\rho^+}{\partial r^+}\right)_{r^+=1,\phi} \quad (7)$$

where r is the distance between the measurement point and the cylinder axes; r_0 is the radius of the porous medium cylinder; $\Delta\rho$ is the density difference between the porous cylinder wall and the surrounding, $\Delta\rho = \rho_w - \rho_f$; D is the mass diffusion coefficient; The dimensionless parameters appearing in this experiment are $\rho^+ = (\rho - \rho_f)/(\rho_w - \rho_f)$, $y^+ = y/r_0$, and $r^+ = r/r_0$, respectively.

EXPERIMENTAL RESULTS AND DISCUSSION

In order to determine the local Sherwood number, it is necessary to measure the local concentration distribution. In the present study, only two typical points (A and C, see fig.1.) are investigated, and the variations of ρ^+ with y^+ (A

and C) for various Re_r are represented in Fig.4 and Fig.5.

It can be seen from the Fig.4 and Fig.5

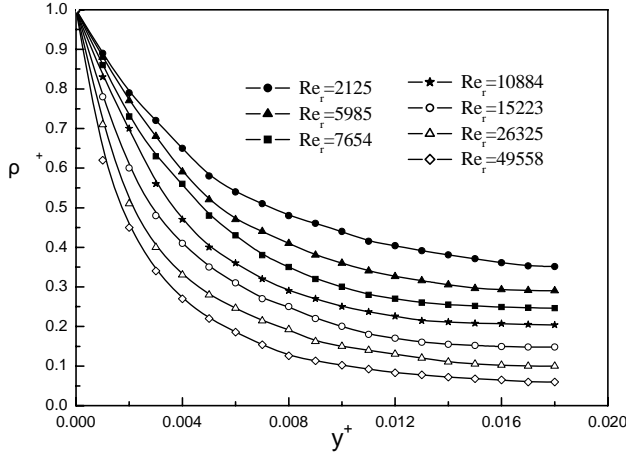


Fig.4 The effect of rotation on the distribution of concentration at point A for various Re_r

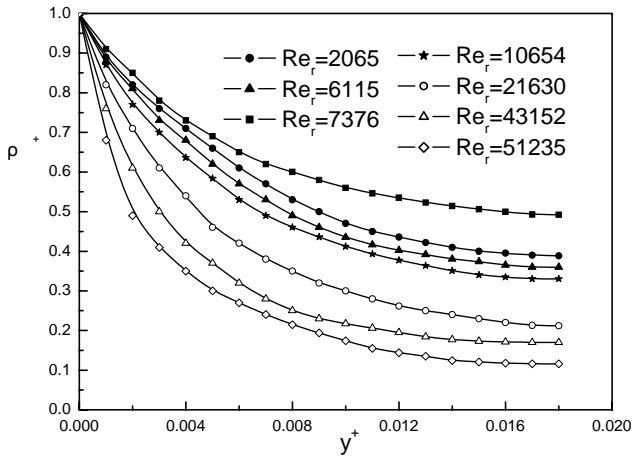


Fig.5 The effect of rotation on the distribution of concentration at point C for various Re_r

that: (1) the concentration gradient at point A is greater than that at point C for the same rotational Reynolds number Re_r , the thickness of boundary layer at point A is thinner than that at point C; (1) on the downstream region at point A, the gradients of concentration increase with the increase of Re_r all the time, while at point C the gradients of concentration decrease with increasing Re_r at first, it reaches a minimum, after that, the gradients of concentration increase with the increase of Re_r ; (3) the results indicate that the effect of rotation on the distribution of concentration consistent with that of temperature around the cylinder reported in literature[5].

The effect of rotation on local mass transfer,

point A and C (see Fig.1.), is also investigated experimentally. A comparison of the variation of the local Sherwood numbers Sh_ϕ with Re_r is shown in Fig6.

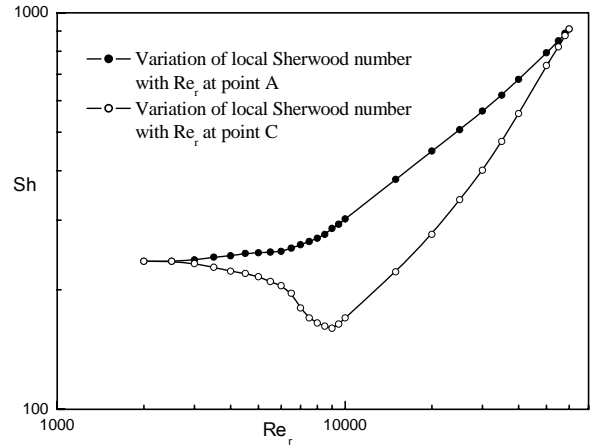


Fig.6 Variation of local Sherwood number Sh_ϕ

with Re_r at point A and point C

The experimental results indicate that the variation of Sh_ϕ with Re_r at point A differs from that at point C. The Sh_ϕ at point A increases with the increase of Re_r all the time, while Sh_ϕ at point C decreases with Re_r increase at low Re_r , as the Re_r increases to 8×10^3 the Sh_ϕ reaches its lowest point. After that point, Sh_ϕ begins to increase with increasing Re_r steeply, the difference of Sh_ϕ between A and C shrinks, and disappears when the rotational Reynolds number Re_r increases to approximately 6×10^4 . The explanation for abovementioned phenomenon is as follows: in the parallel flow region (see Fig.1. D-A-B), the effect of rotation is consistent with the effect of natural convection. They both enhance the mass transfer, as a result, Sh_ϕ increases with increasing Re_r . While in the counter flow region (see Fig.1.B-C-D), the effect of rotation is inconsistent with the natural convection, at low Re_r up to $Re_r = 8 \times 10^3$, Sh_ϕ decreases with increasing Re_r , indicating that the negative effect of rotation is more dominant than that of the positive effect of natural convection. Beyond this region, up to $Re_r = 6 \times 10^4$, with the increase of Re_r , the positive effect of rotation gradually plays a more and more dominant role than that of natural convection, the differences around the

porous cylinder radial angle (φ) reduces, eventually becomes negligible.

The average Sherwood number Sh varying

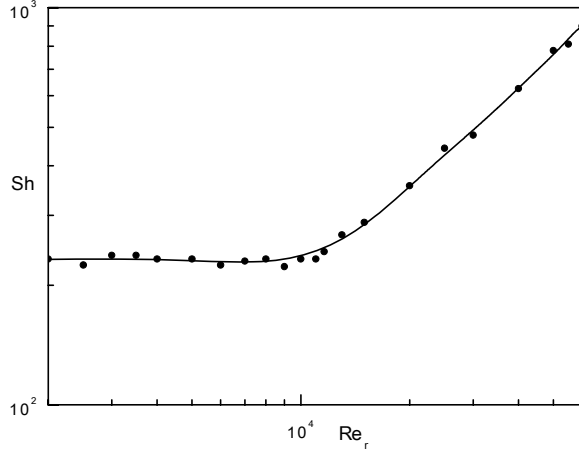


Fig.7 Variation of mean Sh with Re_r

with Re_r is measured by means of the method of calorimeter made from silicon rubber sheet, shown in Fig.7.

Fig.7 indicates that the average Sherwood number Sh variation with Re_r exhibits three different regimes: at low Re_r , up to $Re_r = 7.0 \times 10^3$, Sh is independent of Re_r , during this period, the effect of natural convective mass transfer is more dominant than that of rotation. Beyond this region, up to $Re_r = 1.1 \times 10^4$, the importance of rotation on the mass transfer grows, and the average Sherwood number Sh increases slightly with the increase of Re_r . For $Re_r = 1.1 \times 10^4 - 6.0 \times 10^4$, the effect of rotation on mass transfer is very dominant, Sh increases with increasing Re_r obviously.

The result also indicates that the average Sherwood number Sh measured by means of the calorimeter is larger than the average of the two local Sherwood numbers Sh_φ at point A and point C. The result is similar to that of convective heat transfer reported by X. L [11]. This is mainly because of the influence of heat radiation on the temperature gradient in boundary layer, so that the temperature gradient measured is smaller than it should be, and the local convective mass transfer coefficient h_φ is smaller than the average convective mass transfer coefficient h , and the local Sherwood number Sh_φ is smaller than the

average Sherwood number Sh .

Fig.8 shows the results of the effect of rotation on the mass transfer for different mass flux m . There are four different conditions measured in the paper.

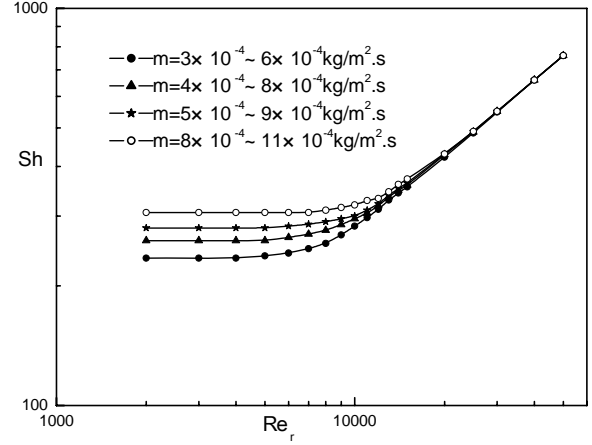


Fig.8 Variation of Sh with Re_r for different mass flux m

The mass transfer curves indicate that the variation of average Sherwood number Sh with Re_r can be divided into two different regimes: when $Re_r \leq Re_{r,cri}$, the average Sherwood number Sh is independent of Re_r , however there is an obvious difference between the average Sherwood numbers Sh for four mass flux m ranges. This is because the effect of rotation can be negligible in comparison to natural convection for a sufficiently small Re_r . For $Re_r > Re_{r,cri}$, the effect of rotation becomes more and more dominant comparing with that of natural convection, as the Re_r increases to large enough, the effect of natural convection becomes so small that it can be negligible in comparison to rotation, and the difference of the four mean Sherwood numbers Sh disappears.

Based on the analysis and the experimental data, the average Sherwood number Sh from a porous medium surface of a horizontal rotating cylinder has been correlated as function of Re_r, Gr_r and Sc , the correlation equation is very useful in the industrial design and engineering applications. In the present experiment, both the natural convection and the forced convection should be covered. Therefore the correlation equation must take the form of

$$Sh = f(Re_r, Gr_r, Sc) \quad (8)$$

By the analogy between the heat and mass transfer, referring to the reported results by X.M Zhang (1987), the mass transfer correlation equation

can be given as follows:

$$Sh = k[(a Re_r^b + Gr).Sc]^p \quad (9)$$

where $k = 0.32$, $p = 1/3$. a and b can be derived from the experimental data as: $a = 8.5$, $b = 2$, thus, the correlation equation is shown as below:

$$Sh = 0.32[(8.5Re_r^2 + Gr).Sc]^{1/3} \quad (10)$$

The experimental data and the correlation equation are represented in a log–log coordinate, shown in Fig.9.

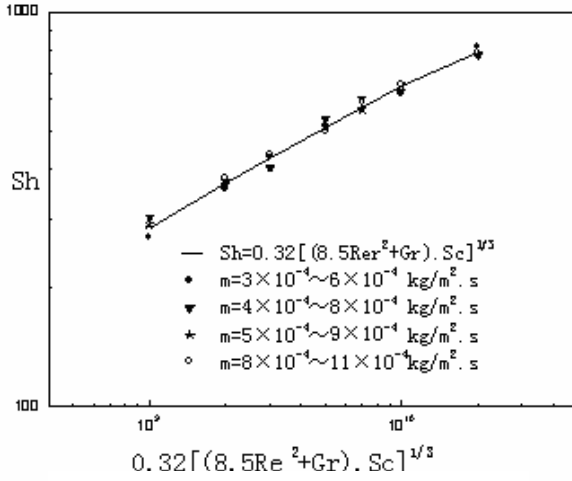


Fig.9 Comparison of equation (10) with experimental data

An error analysis signifies that the mean error between experimental data and the equation (10) is equivalent to approximately 5%. It indicates that equation (10) does provide a reasonable representation of the relationship and a reasonable estimate of the Sherwood number Sh .

According to the equation (10), at very low Re_r , the effect of rotation on the mass transfer is much smaller than natural convection, Sh is independent of Re_r , the effect of rotation can be negligible. This regime is corresponding the level set of the four curves shown in Fig.8. For this region, the equation (10) can be simplified to

$$Sh = 0.32(Gr.Sc)^{1/3} = 0.32Ra^{1/3} \quad (11)$$

Equation (11) shows that the average Sherwood number Sh is independent of Re_r at low Re_r , during this period, the flow around the porous medium cylinder surface maintains lamina, the experimental data and equation(11) are plotted in a log–log coordinate, shown in Fig.10. The error

between equation (11) and experimental data is carried out to be approximately 4.2%. This means that it provides a better prediction for experiments at the low Reynolds number limit, i.e. $Sh \propto Ra^{1/3}$.

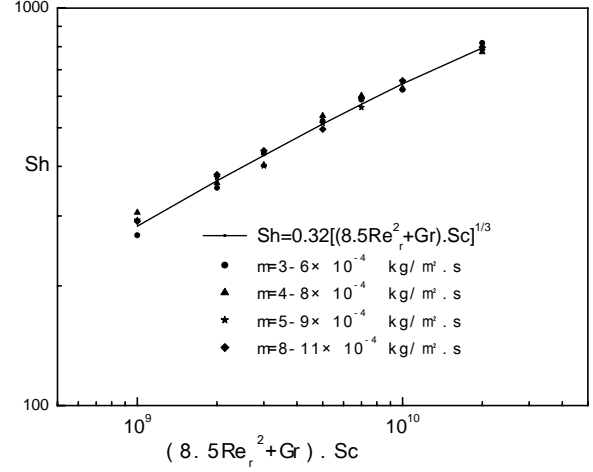


Fig.10 Correlation of Sh with Ra at low Reynolds number for different m

At large Reynolds numbers, the effect of natural convection becomes much more small than rotation, the average Sherwood number Sh is mainly dependent of Re_r , equation (10) can be simplified to:

$$Sh = 0.55 Re_r^{2/3} \quad (12)$$

where the Schmidt number $Sc \approx 0.6$ for vapor diffusion in the air, equation (12) could actually provide a slightly better prediction at higher Reynolds numbers. The error between equation (12) and experimental data is up to approximately 7.3%.

Based on the previous analysis and discussion, at low-Reynolds-number, the Sh can be estimated with equation (11). At large-Reynolds-number, it can be predicated according to equation (12). Which equation is more suitable depending on the critical Reynolds number $Re_{r,cri}$.

In order to obtain the $Re_{r,cri}$, equation (11) is substituted into equation (12)

$$0.32(Gr.Sc)^{1/3} = 0.55 Re_r^{2/3} \quad (13)$$

from which the critical Reynolds number can be derived as follows:

$$Re_{r,cri} = 0.44(Gr.Sc)^{1/2} = 0.44Ra^{1/2} \quad (14)$$

The equation (14) is the critical Reynolds number judgment equation. In the present experiment, the measured critical Reynolds number ranges from $7.0 \times 10^3 - 1.1 \times 10^4$. The previous

experimental performed by X. Li [11] result reported that the heat transfer critical Reynolds number is approximately $Re_{r,cri} = 1.7 \times 10^4$, which is relative larger than the mass transfer critical Reynolds number. The phenomena above is mainly because: (1) The surface roughness from the mass transfer cylinder wall is larger than that from a heat transfer cylinder metal wall, the disturbance is greater than that of the later. (2) The medium of mass transfer boundary layer consists of vapor and air, while the medium of the heat transfer boundary layer consists of only dry air, thus the density and the inertia of the former is greater than that of the later, the centrifugal effect of the former is also greater than that of the later. (3) At the porous medium cylinder wall, the radial mass flux is non-zero, i.e. $m|_{r=r_0} \neq 0$, the deviating velocity of the fluid is larger than that of heat transfer. All the reasons above make the mass transfer critical Reynolds number smaller than that of the heat transfer.

CONCLUSIONS

Based on the study of mass transfer characteristics from the porous medium surface of a rotating cylinder in two dimensions, the following conclusions may be deduced:

(1) The effect of the rotation in the parallel flow region differs from that in the upstream region. In the parallel flow region, Sh_ϕ increase gradually with the increasing Re_r , while in the upstream region, Sh_ϕ decreases as Re_r increases until it hits the minimum. Since then, Sh_ϕ begins to increase with increasing Re_r , the rate of spatial variation of Sh_ϕ becomes steeper, the difference between the parallel flow side Sh_ϕ and the upstream side Sh_ϕ shrinks, and eventually disappears when the Re_r reaches to approximately 6.0×10^4 .

(2) The average Sherwood number Sh measured via the method of calorimeter is slightly greater than the average of the two local Sherwood numbers measured at point A and point C.

(3) At low rotational Reynolds numbers ($Re_r \leq 7 \times 10^3$), the effect of natural convection is more dominant than that of rotation. The effect of rotation on the mass transfer is negligible, and there are obvious differences between Sh for different m regions. However, as the Re_r increase

($7.0 \times 10^3 < Re_r \leq 1.1 \times 10^4$), the effect of rotation increases and the effect of natural convection decreases. At high Reynolds number ($1.1 \times 10^4 < Re_r \leq 6 \times 10^4$), the effect of rotation becomes more and more dominant, the effect of natural convection is gradually negligible.

(4) The Sh has been correlated as function of Re_r , Gr , and Sc for $2.0 \times 10^3 \leq Re_r \leq 6 \times 10^4$. The resultant equation is $Sh = 0.32[(8.5Rr_r^2 + Gr).Sc]^{1/3}$. At low Reynolds numbers, the equation can be simplified to $Sh = 0.32(Gr.Sc)^{1/3} = 0.32Ra^{1/3}$. At large Reynolds numbers, it can be predigested as $Sh = 0.55Re_r^{2/3}$.

(5) In the present experiment, the critical Reynolds number $Re_{r,cri}$ can be related to Gr, Sc or Ra by: $Re_{r,cri} = 0.44(Gr.Sc)^{1/2} = 0.44Ra^{1/2}$. The measured mass transfer $Re_{r,cri}$ ranges from 7.0×10^3 to 1.1×10^4 , which is less than the pure heat transfer critical Reynolds number $Re_{r,cri} = 1.7 \times 10^4$.

REFERENCES

- [1] L. Labraga, T. Berkah, Mass transfer from rotating circular cylinders with and without crossflow, *Int. Journal of Heat and Mass Transfer*, Vol.47,2004,pp.2493-2499.
- [2] X.M.Zhang, W.Y.Li. Convective Heat Transfer from A Horizontal Rotating Cylinder[A]. Heat Transfer Science and Technology[C]. New York: Hemisphere Publishing Corp, 1987. 278-284.
- [3] F. M. Sparrow, S. S. Kang and Z. M. Hossfeld, Heat or mass transfer adjacent to the free end of a rotating cylinder, *Int. J. Heat Mass Transfer*, Vol.30,1987,pp. 807-809.
- [4] K. Bremhorst, G. Kear, A. Keating, S. Huang, Mass Transfer Rate Measurements on a Stepped Rotating Electrode, *Corrosion*, submitted, 2003.
- [5] K. S. Hwang, H. J. Surg, and J. M. Hyun, Mass transfer measurements from a blunt-faced flat plate in a uniform flow, *Int. J. Heat and Fluid Flow*, Vol.17,1996,pp. 178-182.
- [6] G. Kear, A. Purchase, K. Bremhorst, Electrochemical deposition of cupric ions for the determination of mass transfer rates to a stepped rotating cylinder electrode, *Transactions of the Institute of Metal Finishing*, Vol. 81,2003,pp. 141-153.

- [7] M. Bilson, Turbulent Flow and Scalar Transport in the Straight Pipe and Rotating Cylinder, A Comparison of Transport Mechanisms, PhD Thesis, Division of Mechanical Engineering, The University of Queensland, submitted, 2004.
- [8] Fouad A. Youssef, On the heat transfer from an expanding cylinder in cross flow, *Applied Thermal Engineering*, Vol.17,1997,pp.235-248.
- [9] F. Gori, L. Bossi, Optimal slot height in the jet cooling of a circular cylinder, *Applied Thermal Engineering*, Vol.23,2003,pp.859-870.
- [10] Yan Jialu, Zhao Yuzhen, Shang Demin. Specific relative humidity and a generalized enthalpy-humidity chart for moist air[J]. *Journal of Engineering Thermophysics* , 1984, 5(4): 90-93 (in Chinese).
- [11]X. Li, The study of local heat transfer coefficient from a horizontal cylinder, Master thesis, Department of Mechanical engineering, Tianjin University, 1987.
- [12]B.X. Wang,<Engineering Heat and Mass Transfer>,Chinese Science Publishing Company,1998.
- [13] S.N.GUPTA, D.K. Pander & J.K. Singh, Mass Transfer From Rotating Cylinders, *Indian Journal of Technology*,Vol.15,1997,pp.135-138.
- [14] Y.R. Li, D.L. Zeng, S.Y. Wu, The couple heat and mass transfer during the drying of a capillary porous media, *Journal of Engineering Thermophysics*,Vol.20,1999),pp.90-93.
- [15] G. Q. Zhang, Z.M. Jin, Natural Convection with Heat and Mass Transfer in a Porous Media, *Journal of Nanjing University of Science and Technology*,Vol.22,1998,pp.169-172.